

# The Effects of Dark Matter-Baryon Scattering on Redshifted 21 cm Signals

Hiroyuki Tashiro<sup>1</sup>, Kenji Kadota<sup>2</sup> and Joseph Silk<sup>3,4,5</sup>

<sup>1</sup> *Department of Physics, Nagoya University, Nagoya 464-8602, Japan*

<sup>2</sup> *Center for Theoretical Physics of the Universe, Institute for Basic Science, Daejeon 305-811, Korea*

<sup>3</sup> *Institut d'Astrophysique de Paris, CNRS, UPMC Univ Paris 06, UMR7095, 98 bis, boulevard Arago, F-75014, Paris, France*

<sup>4</sup> *The Johns Hopkins University, Department of Physics and Astronomy, Baltimore, Maryland 21218, USA*

<sup>5</sup> *Beecroft Institute of Particle Astrophysics and Cosmology, University of Oxford, Oxford OX1 3RH, UK*

## Abstract

We demonstrate that elastic scattering between dark matter (DM) and baryons can affect the thermal evolution of the intergalactic medium at early epochs and discuss the observational consequences. We show that, due to the interaction between DM and baryons, the baryon temperature is cooled after decoupling from the CMB temperature. We illustrate our findings by calculating the 21 cm power spectrum in coexistence with a velocity-dependent DM elastic scattering cross section. For instance, for a DM mass of 10 GeV, the 21 cm brightness-temperature angular power spectrum can be suppressed by a factor 2 within the currently allowed DM-baryon cross section bounded by the CMB and large-scale structure data. This scale-independent suppression of the angular power spectrum can be even larger for a smaller DM mass with a common cross section (for instance, as large as a factor 10 for  $m_d \sim 1$  GeV), and such an effect would be of great interest for probing the nature of DM in view of forthcoming cosmological surveys.

## 1 Introduction

The nature of dark matter (DM) is one of the greatest mysteries of modern cosmology. One can infer its properties through its interactions with other visible objects. Even though conventional DM models assume only gravitational interactions with ordinary baryonic matter, other forms of couplings are not ruled out and deserve further study in view of the potential signals observable in forthcoming experiments. DM-baryon interactions are of great interest for cosmology because the DM-baryon coupling can modify the evolution of structure formation at early epochs, and stringent constraints have been obtained from current data (e.g. CMB and Ly- $\alpha$ ) for a wide variety of dark matter models such as millicharged DM, dipole DM and strongly interacting DM [1, 2, 3, 4, 5, 6].

In this paper, we focus on the impact of the DM-baryon coupling on the temperature evolution of DM and baryons and explore the consequences for the redshifted 21 cm signal from very early epochs.

In the standard cosmology, the baryon temperature  $T_b$  couples with the CMB temperature  $T_\gamma$  due to Compton scattering via the small residual fraction of free electrons left over from recombination down to a redshift  $z_{\text{dec}} (\sim 200)$  while  $T_b$  subsequently cools adiabatically at lower redshift  $z \lesssim z_{\text{dec}}$ . On the other hand, the DM temperature  $T_d$  decouples from  $T_\gamma$  at a much earlier stage of the universe and  $T_d$  is assumed to evolve adiabatically since then. The DM is hence “cold”, and  $T_d$  is much lower than  $T_b$ . Due to DM-baryon coupling, however, the baryons can be cooled by the DM after the baryon temperature decouples from the CMB temperature. In order to probe this effect, we consider the observations of redshifted 21 cm lines from neutral hydrogen during the dark ages before reionization starts ( $20 \lesssim z \lesssim 1000$ ). The signal of redshifted 21 cm lines depends on the properties of baryon gas at high redshifts: including the density, the temperature and the ionization fraction [7] (see refs. [8, 9] for recent reviews). The observations of redshifted 21 cm lines hence can provide a probe of the thermal evolution of baryonic gas. There have been related papers investigating the 21 cm signal due to energy injection during the dark ages including the dissipation of magnetic fields [10, 11], energy injection from primordial black holes [12, 13], and the decay or annihilation of dark matter [14, 15]. Our study in contrast looks into the effects of elastic scattering between the DM and baryons on the 21 cm signals by quantifying the change in the evolution of  $T_b$  and  $T_d$  due to DM-baryon coupling.

There are several on-going and planned projects to measure the redshifted 21 cm signals by large interferometers such as the LOw Frequency ARray (LOFAR) [16], the Murchison Widefield Array (MWA) [17], the Giant Metre-wave Radio Telescope (GMRT) [18] and Square Kilometer Array (SKA)<sup>1</sup>. The purpose of this paper is to demonstrate the potential significance of DM-baryon coupling on the 21cm observables and investigate the range of DM-baryon coupling for observational feasibility.

We discuss, for simplicity, the case where cold dark matter accounts for the entire DM density, and we calculate the 21 cm signal in the presence of DM-baryon coupling during the dark ages before reionization starts  $20 \lesssim z \lesssim 1000$  for its observational feasibility. This suffices for our purpose of quantifying the significance of DM-baryon coupling on future cosmological observables. Throughout this paper, we adopt the standard  $\Lambda$ CDM model parameters:  $h = 0.7$ ,  $h^2\Omega_b = 0.0226$  and  $\Omega_d = 0.112$ , where  $h$  is the present Hubble constant normalized by 100 km/s/Mpc and  $\Omega_b$  and  $\Omega_d$  are the density parameters of baryons and DM.

## 2 Thermal evolution of baryons and DM with DM-baryon coupling

We solve the Boltzmann equations to follow the background temperature evolution. The coupling between baryons and DM induces momentum transfer between them, and the temperatures of DM

---

<sup>1</sup><http://www.skatelescope.org/>

and baryons,  $T_d$  and  $T_b$ , evolve as [19]

$$(1+z)\frac{dT_d}{dz} = 2T_d + \frac{2m_d}{m_d+m_H}\frac{K_b}{H}(T_d - T_b), \quad (1)$$

$$(1+z)\frac{dT_b}{dz} = 2T_b + \frac{2\mu_b}{m_e}\frac{K_\gamma}{H}(T_b - T_\gamma) + \frac{2\mu_b}{m_d+m_H}\frac{\rho_d}{\rho_b}\frac{K_b}{H}(T_b - T_d), \quad (2)$$

where  $\mu_b \simeq m_H(n_H + 4n_{\text{He}})/(n_H + n_{\text{He}} + n_e)$  is the mean molecular weight of baryons (including free electrons, and H, He ions), and  $K_\gamma$  and  $K_b$  are the momentum transfer rates.  $K_\gamma$  represents the usual Compton collision rate

$$K_\gamma = \frac{4\rho_\gamma}{3\rho_b}n_e\sigma_T, \quad (3)$$

where  $\sigma_T$  is the Thomson scattering cross-section. For  $K_b$ , we consider the general form of cross section which can be velocity dependent parameterized by the baryon-DM relative velocity  $v$

$$\sigma(v) = \sigma_0 v^n, \quad (4)$$

so that the momentum transfer rate  $K_b$  becomes [6]

$$K_b = \frac{c_n \rho_b \sigma_0}{m_H + m_d} \left( \frac{T_b}{m_H} + \frac{T_d}{m_d} \right)^{\frac{n+1}{2}}. \quad (5)$$

The spectral index  $n$  depends on the nature of DM models, for instance,  $n = -1$  corresponds to the Yukawa-type potential DM,  $n = -2, -4$  are respectively for dipole DM and millicharged DM [3, 4, 5, 6, 20, 21, 22, 23, 24, 25, 26]. The constant coefficient  $c_n$  depends on the value of  $n$  and also can include the correction factor for including the helium in addition to hydrogen.  $c_n$  can vary in the range of  $\mathcal{O}(0.1 \sim 10)$  for the parameter range of our interest [6] and we simply set  $c_n = 1$  in our analysis, which suffices for our purpose of demonstrating the effects of the DM-baryon coupling on the 21cm observables<sup>2</sup>.

We solve Eqs. (1) and (2) with  $T_\gamma = T_0(1+z)$ , where  $T_0 = 2.73$  K, numerically. In the early stage of the universe, it is well-known that the baryon temperature is tightly coupled with the CMB temperature,  $T_b \sim T_\gamma$ . Similarly, for a sufficiently large  $K_b$ , the difference between  $T_d$  and  $T_b$  can become small in the early universe. To numerically calculate the evolution accurately in both of these tight coupling regimes, it is useful to expand Eqs. (1) and (2) up to the first order in the temperature differences as performed in Ref. [29]. For this purpose, we introduce two heating time-scales due

---

<sup>2</sup>We in this paper use the conventional cross section for the momentum transfer [5, 6, 27, 28], which is the integration of the differential cross section weighted by  $(1 - \cos\theta)$

$$\sigma(v) = \int d\cos\theta (1 - \cos\theta) \frac{d\sigma(v)}{d\cos\theta} \quad (6)$$

The weight factor  $(1 - \cos\theta)$  is introduced to consider the longitudinal momentum transfer and it can regulate spurious infrared divergence for the forward scattering with no momentum transfer corresponding to  $\cos\theta \rightarrow 1$ .

to Compton scattering and DM-baryon coupling,  $t_C = m_e/2\mu_b K_\gamma$  and  $t_{DB} = (m_d + m_H)/2m_d K_b$ , and we classify the thermal evolution in the early universe in three cases. The first is the case with  $Ht_C \ll 1$  and  $Ht_{DB} \ll 1$ , that is,  $T_b$  and  $T_d$  are tightly coupled with  $T_\gamma$ . The second case is for  $Ht_C \ll 1$  and  $Ht_{DB} > 1$ , in which only  $T_b$  is tightly coupled with  $T_\gamma$ . The third is for  $Ht_C > 1$  and  $Ht_{DB} \ll 1$  (which corresponds to  $z \lesssim z_{\text{dec}}$  for the parameter range of our interests as explicitly shown below).

## 2.1 Regime I: $Ht_C \ll 1$ and $Ht_{DB} \ll 1$

When  $Ht_C \ll 1$  and  $Ht_{DB} \ll 1$ , the difference among  $T_b$ ,  $T_d$  and  $T_\gamma$  would be very small, and we can expand  $T_b$  and  $T_d$  as

$$T_b = T_\gamma - \epsilon_\gamma, \quad (7)$$

$$T_d = T_b - \epsilon_b, \quad (8)$$

where  $|\epsilon_\gamma|/T_\gamma \ll 1$  and  $|\epsilon_b|/T_b \ll 1$ . We also assume that  $\epsilon_\gamma/T_\gamma$  and  $\epsilon_b/T_b$  are of the same order as  $Ht_C$  and  $Ht_{DB}$ .

Substituting Eq. (7) into Eq. (2), we obtain up to first order in  $\epsilon_b$

$$\frac{\epsilon_b}{T_\gamma} = Ht_{DB}, \quad (9)$$

where we used  $T_\gamma \propto (1+z)$ . Because the coefficient  $1/Ht \gg 1$  is very large, we treat  $d\epsilon/dz = 0$  so that  $dT_d/dz = dT_b/dz = dT_\gamma/dz$  at first order. Similarly  $\epsilon_\gamma$  is given by

$$\frac{\epsilon_\gamma}{T_\gamma} = \left(1 + \frac{1}{f}\right) Ht_C, \quad (10)$$

where  $f$  is  $f = m_d \Omega_b / \mu_b \Omega_d$ .

With these approximations at hand, in terms of  $\epsilon_\gamma$  and  $\epsilon_b$ , the time evolutions of the temperature can be rewritten as

$$\frac{dT_b}{dz} \approx \frac{T_\gamma}{1+z} - \epsilon_\gamma \left( \frac{1}{1+z} + \frac{d \ln H}{dz} + \frac{d \ln t_C}{dz} \right), \quad (11)$$

$$\frac{dT_c}{dz} \approx \frac{T_\gamma}{1+z} - \epsilon_\gamma \left( \frac{1}{1+z} + \frac{d \ln H}{dz} + \frac{d \ln t_C}{dz} \right) - \epsilon_b \left( \frac{1}{1+z} + \frac{d \ln H}{dz} + \frac{d \ln t_{DB}}{dz} \right), \quad (12)$$

where we assume that  $f$  is constant<sup>3</sup>. The evolutions of  $T_b$  and  $T_d$  are obtained by solving Eqs. (11) and (12) with Eqs. (9) and (10).

---

<sup>3</sup>Since  $f$  depends on the ionization rate through  $\mu_b$ , this assumption is invalid during the epochs of recombination and reionization. We, however, checked that, even though the evolution of  $f$  itself is not negligible, its effects on the temperature evolution is negligible even during these epochs.

## 2.2 Regime II: $Ht_C \ll 1$ and $Ht_{DB} > 1$

Although the DM temperature  $T_d$  decouples from the baryon temperature  $T_b$ ,  $T_b$  still couples with  $T_\gamma$ . We hence can assume that

$$T_b = T_\gamma - \epsilon_\gamma, \quad (13)$$

with  $|\epsilon_\gamma|/T_\gamma \ll 1$ .

Eq. (2) provides to first order in  $\epsilon_\gamma$

$$\frac{\epsilon_\gamma}{T_\gamma} = Ht_C + \frac{t_C}{ft_{DB}} \left(1 - \frac{T_c}{T_\gamma}\right). \quad (14)$$

The redshift derivative of  $T_b$  can then be approximated as

$$\frac{dT_b}{dz} \approx \frac{T_\gamma}{1+z} - \frac{T_\gamma}{1+z} Ht_C - T_\gamma t_C \frac{dH}{dz} - T_\gamma H \frac{dt_C}{dz} - \frac{d}{dz} \left[ T_\gamma \frac{t_C}{ft_{DB}} \left(1 - \frac{T_c}{T_\gamma}\right) \right]. \quad (15)$$

We numerically calculate the thermal evolution of  $T_b$  and  $T_d$  from Eq. (15) along with Eq. (1).

## 2.3 Regime III: $Ht_C > 1$ and $Ht_{DB} \ll 1$

In this case, while the baryon temperature  $T_b$  is already decoupled from the CMB temperature  $T_\gamma$ , the dark matter temperature  $T_d$  is coupled to  $T_b$ . We can write the dark matter temperature as

$$T_d = T_b - \epsilon_b, \quad (16)$$

with  $|\epsilon_b|/T_b \ll 1$ . From Eqs. (1) and (2), we obtain to first order in  $\epsilon_b$  and  $Ht_{DB}$ ,

$$\epsilon_b = - \left(1 + \frac{1}{f}\right)^{-1} \frac{t_{DB}}{t_C} (T_b - T_\gamma). \quad (17)$$

Therefore, in this tight-coupling regime, the evolution of  $T_d$  can be approximated as

$$\frac{dT_d}{dz} \approx \frac{dT_b}{dz} - \epsilon_b \left[ \frac{d \ln t_{DB}}{dz} - \frac{d \ln t_C}{dz} + \frac{1}{T_b - T_\gamma} \left( \frac{dT_b}{dz} - \frac{T_\gamma}{1+z} \right) \right]. \quad (18)$$

On the other hand, the evolution of  $T_b$  can be written as

$$(1+z) \frac{dT_b}{dz} \approx 2T_b + \left(1 + \frac{1}{f}\right)^{-1} \frac{1}{Ht_C} (T_b - T_\gamma). \quad (19)$$

Since  $f \propto m_d/m_H$ , the change of  $T_b$  due to the DM-baryon coupling becomes bigger for a bigger  $m_d$  (with a fixed  $\Omega_d$ ), and, in the limit of  $m_d \gg m_H$ , the baryons and DM can be described as a single gas. In such a tight coupling limit with  $m_d \gg m_H$ , the total number density of the DM-baryon mixed gas does not change from that of the baryon gas, and the evolution of  $T_b$  along with a large  $m_d$  is similar to the  $T_b$  evolution without the DM-baryon coupling. In other words, a small  $m_d$  ( $\ll m_H$ ) leads to a significant increase of the total number density of the mixed gas, and the Compton cooling term to couple  $T_b$  to  $T_\gamma$  effectively becomes small. Hence, for a smaller  $m_d$ , the deviation of  $T_b \approx T_d$  from  $T_\gamma$  with the DM-baryon coupling becomes bigger compared with the deviation of  $T_b$  from  $T_\gamma$  without DM-baryon coupling.

### 3 Numerical results for DM and baryon temperature evolution

Following the previous section on numerical treatments of tight coupling regimes, we numerically calculate the DM and baryon temperatures,  $T_d$  and  $T_b$ , modifying the public code `RECFAST` [30]. Before presenting the results with different couplings between DM and baryons, we note that there exist strong constraints on this DM-baryon coupling notably from the CMB and large-scale structure due to the suppression of the matter density perturbations where the DM perturbation growth is suppressed because of the drag force arising from the momentum transfer between the DM and baryon fluids [2, 6, 31, 32]. For instance, small-scale observations (Lyman- $\alpha$  forest) by SDSS and the CMB data by Planck can set upper bounds on the coupling between DM and baryons of order  $\sigma_0/m_d \lesssim 10^{-17,-9,-6,-3,+4} \text{ cm}^2/\text{g}$  for  $n = -4, -2, -1, 0, +2$  [6]. For the purpose of presenting our findings through a concrete example, in the following we discuss the scenarios of  $n = -4$  (typical for a millicharged DM scenario [4, 5, 20, 21, 23]) because a large negative power leads to a prominent enhancement in the cross section for a smaller momentum transfer at low redshift. We found, for the scenarios with  $n = -2, -1, 0, +2$ , that the DM-baryon coupling cannot lead to any appreciable change in the 21 cm power spectrum within the aforementioned cross-section upper bounds from the currently available data.

Fig. 1 represents the temperature evolution with  $n = -4$  for different values of  $\sigma_{17}$ , where we normalized the coupling constant as  $\sigma_0 = \sigma_{17}m_H \times 10^{-17} \text{ cm}^2/\text{g}$ . To demonstrate the mass dependence, we simply show the results for  $m_d = m_H$  and  $10m_H$  in Fig. 1 for different values of DM-baryon coupling. At high redshifts,  $z > z_{\text{dec}}$ ,  $T_b$  is tightly coupled to  $T_\gamma$  ( $T_b \approx T_\gamma$ , and hence the thermal evolution can be described with the treatment in in Sec. 2.2 where  $T_d \propto 1/t_{DB}$ ). It is consequently difficult to find any difference between the evolution of  $T_b$  for the different couplings in Fig. 1 at high redshift. Note, however, that  $T_d$  deviates from  $T_b \approx T_\gamma$  at high redshifts. In the presence of DM-baryon coupling, the DM thermal evolution is not adiabatic and is determined by the balance between the adiabatic cooling and the heating due to the coupling. We can infer, by substituting  $T_b \approx T_\gamma$  in Eq. (1), that DM evolution follows  $T_d \sim T_\gamma/t_{DB}H$ . More precisely, from Fig. 1, we numerically find that the DM temperature is well approximated by the fitting formula  $T_d \approx T_\gamma/1.5t_{DB}H$ . The time-scale  $t_{DB}$  is proportional to  $(m_d + m_H)^2/\sigma_{17}m_d$ . When  $m_d \gg m_H$ ,  $t_{DB} \propto m_d$  which results in  $T_d \propto 1/t_{DB} \propto 1/m_d$ , and Fig. 1 indeed shows that  $T_d$  is larger for a smaller  $m_d$ .

Let us here note that the DM-baryon momentum transfer rate  $K_b$  given in Eq. 5, hence the thermal evolution at high redshifts, turns out to be heavily dependent on  $T_b$  but not so much on  $T_d$ , where the temperature dependence of  $K_b$  shows up in the factor  $(T_b/m_H + T_d/m_d)$ . For  $m_d \gg m_H$ ,  $(T_b/m_H + T_d/m_d) \sim T_b/m_H$  to leading order in  $m_H/m_d$ . For  $m_d \ll m_H$  on the other hand,  $T_d \sim 1/t_{DB} \sim m_d$  and the  $m_d$  dependence cancels out in  $T_d/m_d^4$ .

---

<sup>4</sup>Consequently, because the baryon temperature never exceeds the cold dark matter temperature, this factor  $(T_b/m_H + T_d/m_d)$  would be at most of order  $\sim 2 \times T_b/m_H$  saturated at  $m_d \sim m_H$ . We hence expect the upper bound  $\sigma_0 \lesssim 10^{-16}m_H \text{ cm}^2/\text{g}$  (corresponding to  $\sigma_{17} = 10$  in our notation) which Ref. [6] obtained for  $m_d = 10 \text{ GeV}$  would not become significantly tighter even for a smaller dark matter mass. We therefore restricted the parameter range of our discussion to be  $\sigma_{17} \leq 10$  and presented the results for  $m_d = 10, 1 \text{ GeV}$ , which would suffice our purpose of

At low redshifts after  $T_b$  has decoupled from  $T_\gamma$ ,  $z \lesssim z_{\text{dec}}$ , the coupling between baryons and dark matter affects the temperature evolution of baryons. The baryons become cooler through the DM-baryon coupling because  $T_d < T_b$  as compared with no-coupling scenarios. Sufficient coupling can make the temperatures of baryons and DM equal. Once they match each other, the coupling term in the Boltzmann equations ( $\propto (T_b - T_d)$ ) reaches effectively zero and the thermal evolution becomes adiabatic, that is,  $T_b$  and  $T_d$  are proportional to  $(1+z)^{-2}$  because the DM and baryons have the same adiabatic index. Since we set  $n = -4$  for the velocity-dependence of the coupling, the coupling strength becomes bigger for a smaller momentum transfer at a smaller redshift. The evolution of  $T_b$  is modified at lower redshifts even for a small  $\sigma_{17}$  for  $m_d = m_H$  in the left panel. We find, however, that, when  $\sigma_{17} < 0.001$ , the baryon temperature does not couple with the dark matter temperature even at lower redshifts and its evolution is similar to the case without the coupling. The DM-baryon coupling term for the baryon temperature evolution, which appears in Eq. (2), becomes small with increase of  $m_d$ , as confirmed in Fig. 1.

For a sufficiently large value of DM-baryon coupling (in our example, for  $\sigma_{17} > 10$ ), the DM temperature is well coupled with the baryon temperature, and  $T_d \approx T_b$  is established even around the epoch when the baryon temperature starts to decouple from the CMB temperature. The evolution in this regime corresponds to the tight-coupling case discussed in Sec. 2.3 where a small DM mass, due to a small Compton coupling between  $T_b$  and  $T_\gamma$ , leads to the early decoupling of  $T_b \approx T_d$  from  $T_\gamma$ . The difference of the baryon temperature evolution from the no DM-baryon coupling scenarios hence becomes bigger for a smaller DM mass.

Finally it is worth mentioning the case in the limit of  $m_d \ll m_H$ . At high redshifts  $z > z_{\text{dec}}$ , the time scale  $t_{DB}$  is proportional to  $1/m_d$ , and the DM temperature  $T_d \propto 1/t_{DB}$  which decreases as  $m_d$  becomes small.

The DM-baryon coupling term in Eq. (2) does not become small in the limit of  $m_d \ll m_H$ , in contrast to  $m_d \gg m_H$  case, and, in fact, becomes independent of  $m_d$  with only its dependence on  $\sigma_0$ . Hence the baryon temperature can be dragged to the lower dark matter temperature, and one finds that the change in the  $T_b$  evolution is bigger for a smaller  $m_d$ .

## 4 The evolution of 21 cm signals with DM-baryon coupling

The DM-baryon coupling can affect the evolution of the baryon temperature as shown in the previous section, and the measurement of baryon temperature in the dark ages, in particular during  $20 < z < z_{\text{dec}}$ , could well reveal the nature of DM. The measurement of redshifted 21 cm lines from neutral hydrogen is expected to be a good probe of baryon gas in the dark ages. The strength of the emission or absorption of the 21 cm lines depends on the density, temperature and ionization fraction of baryon gas.

The observational signals of redshifted 21 cm lines are measured as the difference between the brightness temperature of redshifted 21 cm signals and the CMB temperature. This differential

---

showing the potential significance of the DM-baryon coupling on the 21 cm signals.

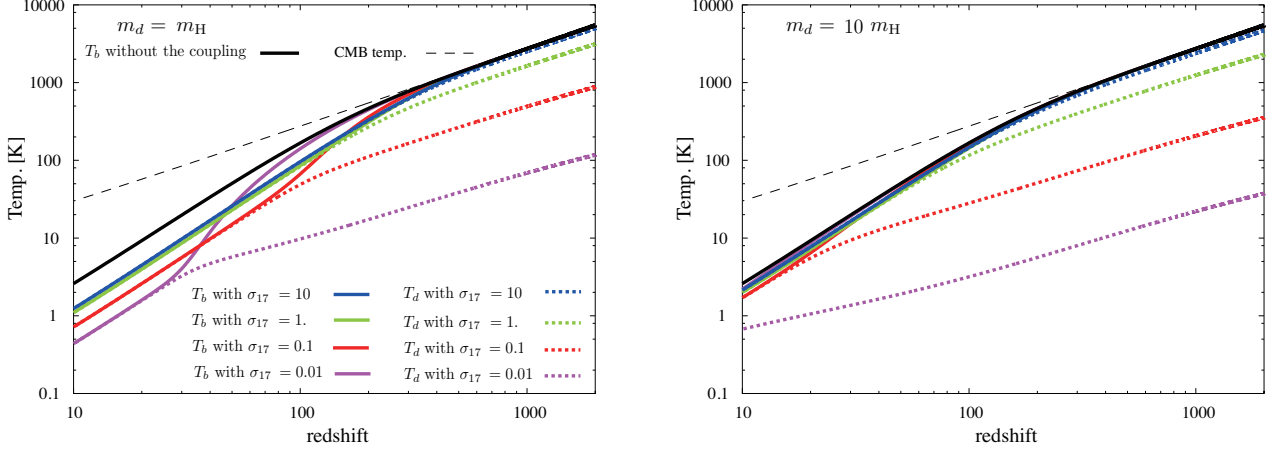


Figure 1: The baryon and dark matter temperature evolution for different values of DM-baryon coupling (the DM-baryon elastic scattering cross section is parameterized as  $\sigma = \sigma_0 v^{-4}$ , with  $\sigma_0 = \sigma_{17} m_H 10^{-17} \text{cm}^2/\text{g}$ ). We set  $m_d = m_H$  in the left panel and  $m_d = 10 m_H$  in the right panel. The solid and dotted lines represent the baryon and dark matter temperatures, respectively. The CMB temperature is plotted as the dashed line. The magenta, red, green and blue lines are for  $\sigma_{17} = 0.01, 0.1, 1.0$  and  $10$  respectively. The black solid line shows the baryon temperature evolution without DM-baryon coupling ( $\sigma_{17} = 0$ ).

brightness temperature is given by

$$\delta T_b(z) = [1 - \exp(-\tau)] \frac{T_s - T_\gamma}{1 + z}, \quad (20)$$

where  $\tau$  is the optical depth and  $T_s$  is the spin temperature. The spin temperature describes the number density ratio of hydrogen atoms in the excitation state to those in the ground state, and is given by [33, 34]

$$T_s = \frac{T_* + T_\gamma + y_k T_b}{1 + y_k}, \quad (21)$$

where  $T_*$  is the temperature corresponding to the energy of hyperfine structure of neutral hydrogen and  $y_k$  represents the kinetic coupling term given by

$$y_k = \frac{T_*}{AT_b} (C_H + C_e + C_p), \quad (22)$$

where  $A$  is the spontaneous emission rate and  $C_H$ ,  $C_e$ , and  $C_p$  are the de-excitation rates of the triplet due to collisions with neutral atoms, electrons, and protons [8]. For these rates, following Ref. [35], we adopt the values from Refs. [8, 36]. Since we are interested in the signals from the dark age, we neglect the Lyman- $\alpha$  coupling (Wouthysen field effect) term [33, 37] in Eq. (21), which is ineffective without luminous objects.

We show the evolution of  $T_s$  for different DM-baryon coupling values in Fig. 2. As one can expect from Fig. 1, the difference from the case without the coupling is larger for  $m_d = m_H$  than



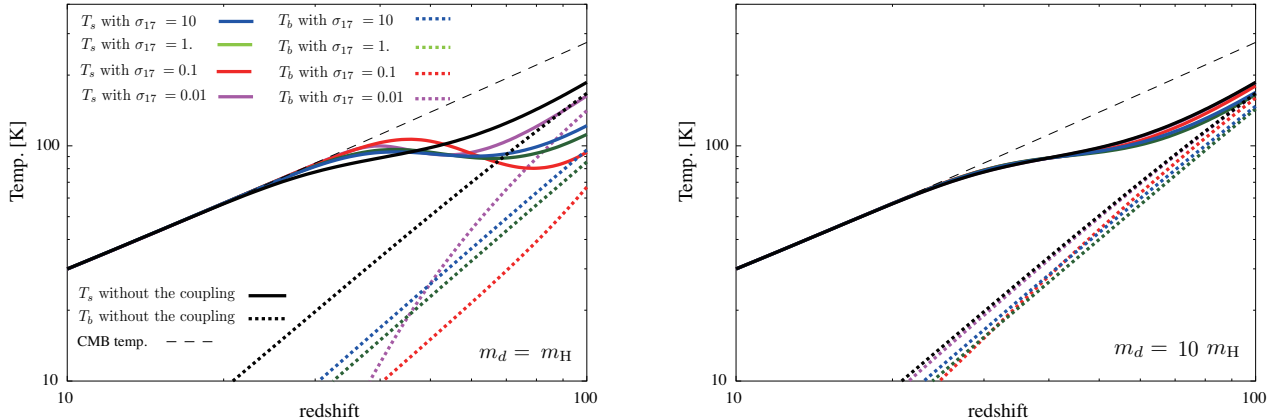


Figure 2: The spin temperature evolution for different values of DM-baryon coupling. The solid, dotted and dashed lines represent the spin, baryon and CMB temperatures, respectively. We set  $m_d = m_H$  in the left panel and  $m_d = 10m_H$  in the right panel. The magenta, red, green and blue lines are for  $\sigma_{17} = 0.01, 0.1, 1.0$  and  $10$  respectively. The temperatures evolution without DM-baryon coupling ( $\sigma_{17} = 0$ ) is plotted in black.

for  $m_d = 10m_H$ . The 21 cm signals depend on  $T_s$ , and we hence can expect the redshift evolution of the differential brightness temperature also depends on  $\sigma_{17}$ .

Measurements of cosmological 21 cm signals will be performed by interferometers such as LOFAR and SKA which can measure the fluctuations in the differential brightness temperature. The angular power spectrum of  $\delta T_b$  is given by

$$C_\ell(z) = \delta T_{b0}^2 \int dk k^2 \Delta_{21,\ell}^2(z, k) P(k), \quad (23)$$

where  $\Delta_{21,\ell}$  is the transfer function for the 21 cm fluctuations,  $P(k)$  is the power spectrum of the primordial curvature perturbations and  $\delta T_{b0}$  is the value of the differential 21cm brightness temperature which can be approximated by [38]

$$\delta T_{b0} \approx 26 \text{ mK } x_H \left(1 - \frac{T_\gamma}{T_s}\right) \left(\frac{h^2 \Omega_b}{0.02}\right) \left[\left(\frac{1+z}{10}\right) \left(\frac{0.3}{\Omega_m}\right)\right]. \quad (24)$$

In this paper, since we consider the effect of the coupling between baryons and dark matter on the temperature evolution, we focus only on the modification of  $\delta T_{b0}$  due to the coupling. We ignore the effect of the DM-baryon coupling on the evolution of the density fluctuations [6, 2]. Therefore, the transfer function  $\Delta_{21,\ell}$ , which we calculate by using CAMB [35], is the same as that in the standard  $\Lambda$ CDM model.

We show the dependence of the angular power spectrum  $C_\ell(z)$  on DM-baryon coupling in Fig. 3. According to Eq. (24), the evolution of  $\delta T_{b0}$  depends on the spin temperature shown in Fig. 2. The coupling between baryons and dark matter lowers the baryon temperature. Therefore, the kinetic coupling term for the hyper-fine structure in Eq. (21) becomes small due to the low baryon temperature. The spin temperature then quickly approaches the CMB temperature for  $z \lesssim 50$ ,

which results in a smaller amplitude of  $C_\ell$  compared with the no coupling case. For instance, for  $\sigma_{17} < 0.1$  with  $m_d = m_H$ , the amplitude of  $C_\ell$  is suppressed by 1/10 (see the red and magenta lines in the left panel of Fig. 3). As the coupling increases, the dark matter temperature becomes larger and approaches the baryon temperature as shown in Fig.1. Fig. 3 indeed shows that the amplitudes are comparable, except in the small coupling case ( $\sigma_{17} = 0.01$ ). The behavior for this small cross-section is due to the fact that  $T_b$  turns out not to couple with  $T_d$  at high redshifts  $z > 50$  due to the small coupling. As  $T_b$  becomes smaller at lower redshifts, however, the coupling can become more effective due to the enhancement for small momentum transfer. Fig. 3 confirms our expectation that the effects of DM-baryon coupling on the  $T_b$  evolution becomes small as  $m_d$  increases (as mentioned at the end of §2.3).

Note that, while the amplitude of  $C_\ell$  is suppressed due to the coupling between baryons and dark matter at a low redshift ( $z \lesssim 40$ ), it is amplified at a high redshift ( $z \gtrsim 50$ ). This is because, at high redshifts, the kinematic coupling term in Eq. (21) is significant and the spin temperature is tightly coupled with the baryon temperature. The deviation of the spin temperature from the CMB temperature hence becomes large and  $C_\ell$  is consequently amplified at high redshifts.

Let us also comment on  $C_\ell$  when  $m_d$  is smaller than  $m_H$ . As mentioned in Sec. 3, the baryon temperature is strongly dragged to the dark matter temperature which becomes small with decreasing  $m_d$ . Therefore, the kinetic coupling term is small for a small  $m_d$  and the spin temperature has a tighter coupling with the CMB temperature. This tight coupling causes the strong suppression of  $C_\ell$ , according to Eq. (24). As a result, when  $m_d \ll m_H$ , the suppression due to the coupling is significant even at large redshifts.

## 5 Discussion and conclusion

Before concluding our studies on 21 cm signals, let us briefly mention other relevant observables which could potentially be affected by the change in the background temperature evolution because of the DM-baryon coupling.

**Epoch of recombination and CMB anisotropies:** If the baryon temperature changes around the epoch of recombination, the last scattering surface could be modified and this modification can produce a footprint on the CMB temperature anisotropies. We evaluate the ionization fraction for different  $\sigma_{17}$  and plot the results in Fig. 4. We found, since the baryon temperature is strongly coupled with the CMB temperature around these redshifts (see Fig. 1), the dark matter cooling cannot decrease the baryon temperature enough to modify the epoch of recombination. Therefore, the coupling between baryons and dark matter cannot produce a observable signature in the primordial CMB anisotropies.

At lower redshifts, when the baryon temperature decouples from the CMB temperature, the dark matter cooling could affect the thermal evolution of baryons. Since the baryon temperature is dragged to lower temperature, the residual ionization fraction becomes small. It is, however, difficult to measure such small residual ionization fraction by cosmological observations.

**CMB distortions:** Precise measurements of CMB spectral distortions from the blackbody spectrum can be a promising probe of thermal history of the Universe (see Ref. [39] for a recent review). Generally CMB distortions can be classified into two types [40, 41]. One is the  $\mu$ -type

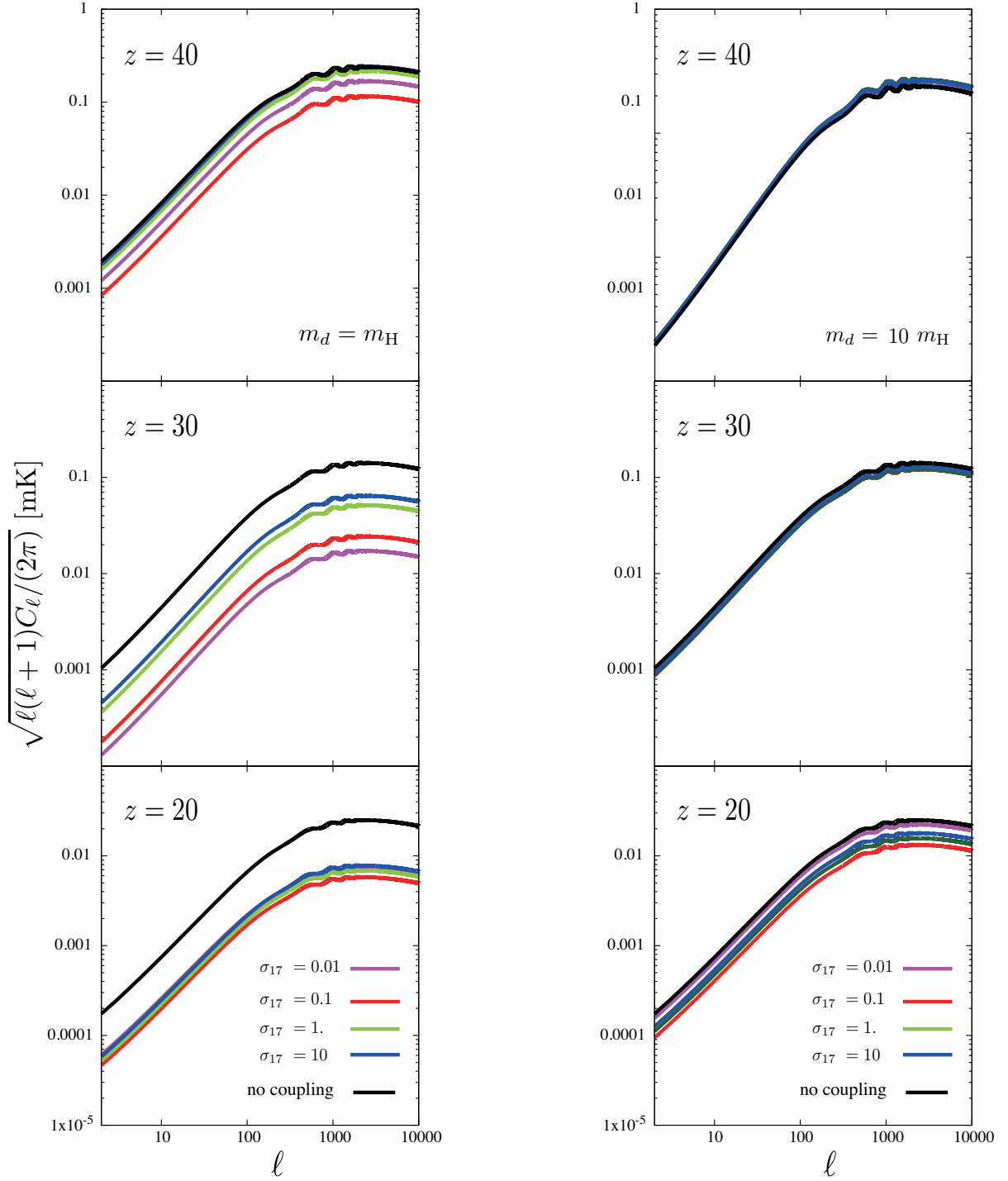


Figure 3: The evolution of the angular power spectrum  $C_\ell$  for different values of DM-baryon coupling. We set  $m_d = m_H$  and  $10m_H$  in the left and right panels, respectively. In both left and right panels, the redshifts are set to  $z = 40$ ,  $30$  and  $20$  from the top to bottom, respectively.

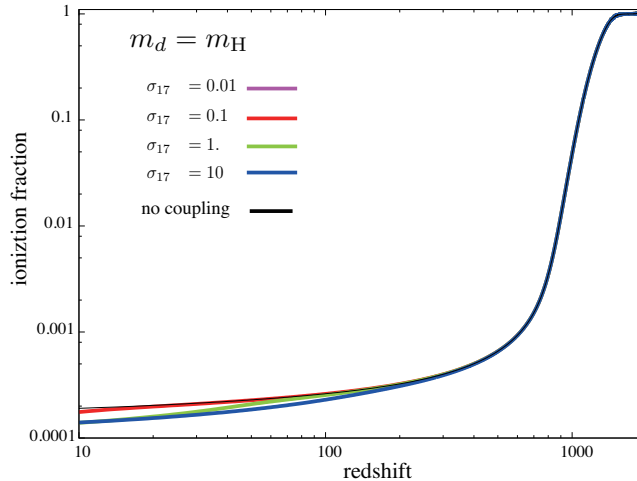


Figure 4: The evolution of the ionization fraction for different values of DM-baryon coupling.

distortion which is generated between  $z \sim 10^6$  and  $z \sim 10^4$ . The other is the  $y$ -type distortion which is produced after the epoch of the  $\mu$ -type distortion generation ( $z \lesssim 10^4$ ).

The difference in the adiabatic indexes between baryons and CMB photons can create CMB distortions [42]. Because the baryon temperature is always lower than the CMB temperature, the energy of the CMB photons is transferred to baryons via Compton scatterings. This energy transfer modifies the CMB frequency spectrum and we can observe this modification as CMB distortions. Following Ref. [42], in order to evaluate the CMB distortions due to this baryon cooling, it is useful to define the parameter  $Y_{\text{BEC}}$  as

$$Y_{\text{BEC}} = - \int dz \left( 1 - \frac{T_b}{T_\gamma} \right) \frac{k_B \sigma_T}{m_e c} \frac{n_e T_\gamma}{(1+z)H}. \quad (25)$$

For example, the  $y$ -parameter which characterizes the  $y$ -type distortion is obtained by  $y = -Y_{\text{BEC}}$ .

We evaluated  $Y_{\text{BEC}}$  for different values of  $\sigma_{17}$ . We find that  $Y_{\text{BEC}}$  becomes at most  $\mathcal{O}(10^{-9})$  for the parameter range of interest,  $10^{-3} < \sigma_{17} < 10^2$ , while  $Y_{\text{BEC}}$  is on the order of  $10^{-10}$  without the coupling between baryons and dark matter. The value of  $Y_{\text{BEC}}$  corresponds to  $\mu \sim 10^{-9}$  for the  $\mu$ -type distortion and  $y \sim 10^{-9}$  for the  $y$ -type distortion. Because the Silk damping of the primordial density perturbations produces  $\mu \sim 10^{-8}$  [43, 44] and the reionization process gives  $y \sim 10^{-7}$  [45], it would be difficult to find the signature of the coupling between baryons and dark matter in the CMB distortions.

We have demonstrated that DM-baryon coupling can affect the background temperature evolution and consequently the 21 cm signal. Our specific example, the velocity-dependent elastic scattering cross-section, would be also of great interest for particle physics studies because of its infrared enhancement for a low momentum transfer, which has been explored for potential signals beyond the standard model at collider and dark matter search experiments [21, 23, 24, 25, 26]. Such probes of

the dark matter properties from both cosmology and particle physics deserve further study in view of forthcoming experiments which can explore the nature of the DM coupling to ordinary baryons.

We have shown that the 21 cm signal is suppressed due to the existence of DM-baryon coupling, and it would certainly be useful to provide further constraints on DM-baryon coupling. For instance, we have found that the 21 cm brightness temperature angular power spectrum can be suppressed by a factor 2 for  $m_d = 10$  GeV within the current bounds from the CMB and Ly- $\alpha$  data. This overall suppression can even be larger for a smaller dark mass with a fixed cross-section, for instance of order a factor 10 for  $m_d = 1$  GeV. We have however found that the degree of further suppression becomes milder for an even smaller  $m_d \ll m_H$ , partly because the temperature dependence of the DM-baryon momentum transfer rate  $K_b$  on the dark matter mass saturates at  $m_d \sim m_H$  and becomes independent of  $m_d$  for  $m_d \ll m_H$ .

We plan to explore the effects of DM-baryon coupling on the evolution of fluctuations in future work where one needs extra care in the treatment of non-linearities. Some simplifications made in our analysis would also deserve further study. For instance, we considered only the thermal velocity and did not include the peculiar velocity contributions in estimating the DM-baryon momentum transfer rate. Even though the inclusion of such bulk velocity contributions does not always change the constraints on the upper bounds on the allowed DM-baryon scattering cross sections, there are cases where the cross-section constraints could get tighter (possibly even by a factor 10) even though more detailed numerical analysis is needed because of the uncertainties caused by non-linear evolution [6].

This work was supported by the MEXT of Japan, Program for Leading Graduate Schools "PhD professional: Gateway to Success in Frontier Asia", the Japan Society for Promotion of Science (JSPS) Grant-in-Aid for Scientific Research (No. 25287057), the ERC project 267117 (DARK) hosted by Université Pierre et Marie Curie - Paris 6 and at JHU by NSF grant OIA-1124403.

## References

- [1] D. N. Spergel and P. J. Steinhardt, Phys. Rev. Lett. **84**, 3760 (2000) [astro-ph/9909386].
- [2] X. -l. Chen, S. Hannestad and R. J. Scherrer, Phys. Rev. D **65**, 123515 (2002) [astro-ph/0202496].
- [3] K. Sigurdson, M. Doran, A. Kurylov, R. R. Caldwell and M. Kamionkowski, Phys. Rev. D **70**, 083501 (2004) [Erratum-ibid. D **73**, 089903 (2006)] [astro-ph/0406355].
- [4] A. Melchiorri, A. Polosa and A. Strumia, Phys. Lett. B **650**, 416 (2007) [hep-ph/0703144].
- [5] S. Tulin, H. -B. Yu and K. M. Zurek, Phys. Rev. D **87**, no. 11, 115007 (2013) [arXiv:1302.3898 [hep-ph]].
- [6] C. Dvorkin, K. Blum and M. Kamionkowski, Phys. Rev. D **89**, 023519 (2014) [arXiv:1311.2937 [astro-ph.CO]].

- [7] P. Madau, A. Meiksin and M. J. Rees, *Astrophys. J.* **475**, 429 (1997) [astro-ph/9608010].
- [8] S. Furlanetto, S. P. Oh and F. Briggs, *Phys. Rept.* **433**, 181 (2006) [astro-ph/0608032].
- [9] J. R. Pritchard and A. Loeb, *Rept. Prog. Phys.* **75**, 086901 (2012) [arXiv:1109.6012 [astro-ph.CO]].
- [10] H. Tashiro and N. Sugiyama, *Mon. Not. Roy. Astron. Soc.* **372**, 1060 (2006) [astro-ph/0607169].
- [11] M. Shiraishi, H. Tashiro and K. Ichiki, *Phys. Rev. D* **89**, 103522 (2014) [arXiv:1403.2608 [astro-ph.CO]].
- [12] K. J. Mack and D. H. Wesley, arXiv:0805.1531 [astro-ph].
- [13] H. Tashiro and N. Sugiyama, *Mon. Not. Roy. Astron. Soc.* **435**, 3001 (2013) arXiv:1207.6405 [astro-ph.CO].
- [14] S. R. Furlanetto, S. P. Oh and E. Pierpaoli, *Phys. Rev. D* **74**, 103502 (2006) [astro-ph/0608385].
- [15] L. Chuzhoy, arXiv:0710.1856 [astro-ph].
- [16] M. P. van Haarlem, M. W. Wise, A. W. Gunst, G. Heald, J. P. McKean, J. W. T. Hessels, A. G. de Bruyn and R. Nijboer *et al.*, *Astronomy & Astrophysics*, **556**, 53 (2013) arXiv:1305.3550 [astro-ph.IM].
- [17] C. J. Lonsdale, R. J. Cappallo, M. F. Morales, F. H. Briggs, L. Benkevitch, J. D. Bowman, J. D. Bunton and S. Burns *et al.*, *Proceedings of the IEEE*, **97**, 1497 (2009) arXiv:0903.1828 [astro-ph.IM].
- [18] G. Paciga, J. Albert, K. Bandura, T. -C. Chang, Y. Gupta, C. Hirata, J. Odegova and U. -L. Pen *et al.*, arXiv:1301.5906 [astro-ph.CO].
- [19] C. -P. Ma and E. Bertschinger, *Astrophys. J.* **455**, 7 (1995) [astro-ph/9506072].
- [20] S. Davidson, S. Hannestad and G. Raffelt, *JHEP* **0005**, 003 (2000) [hep-ph/0001179].
- [21] D. Feldman, Z. Liu and P. Nath, *Phys. Rev. D* **75**, 115001 (2007) [hep-ph/0702123 [HEP-PH]].
- [22] E. Masso, S. Mohanty, S. Rao *Phys. Rev. D* **80**, 036009 (2009) [arXiv:0906.1979 [hep-ph]].
- [23] S. D. McDermott, H. -B. Yu and K. M. Zurek, *Phys. Rev. D* **83**, 063509 (2011) [arXiv:1011.2907 [hep-ph]].
- [24] I. Lopes, K. Kadota and J. Silk, *Astrophys. J. Lett.* **780**, L15 (2014) [arXiv:1310.0673 [astro-ph.SR]].
- [25] E. Del Nobile, G. B. Gelmini, P. Gondolo and J. -H. Huh, *JCAP* **1406**, 002 (2014) [arXiv:1401.4508 [hep-ph]].

- [26] K. Kadota and J. Silk, Phys. Rev. D **89**, 103528 (2014) [arXiv:1402.7295 [hep-ph]].
- [27] S. A. Raby and G. West, Nucl. Phys. B **292**, 793 (1987).
- [28] P. Krstić and D. Schultz, Phys. Rev. A **60** 2118 (1999)
- [29] D. Scott and A. Moss, arXiv:0902.3438 [astro-ph.CO].
- [30] S. Seager, D. D. Sasselov and D. Scott, Astrophys. J. **523**, L1 (1999) [astro-ph/9909275].
- [31] B. D. Wandelt, R. Dave, G. R. Farrar, P. C. McGuire, D. N. Spergel and P. J. Steinhardt, astro-ph/0006344.
- [32] S. Davidson, S. Hannestad and G. Raffelt, JHEP **0005**, 003 (2000) [hep-ph/0001179].
- [33] G. B. Field, Proc. I.R.E. **46**, 240 (1958).
- [34] G. B. Field, Astrophys. J. **129**, 536 (1959).
- [35] A. Lewis and A. Challinor, Phys. Rev. D **76**, 083005 (2007) [astro-ph/0702600 [ASTRO-PH]].
- [36] S. Furlanetto and M. Furlanetto, Mon. Not. Roy. Astron. Soc. **379**, 130 (2007) [astro-ph/0702487 [ASTRO-PH]].
- [37] S. A. Wouthuysen, Astron. J. **57**, 31 (1952).
- [38] B. Ciardi and P. Madau, Astrophys. J. **596**, 1 (2003) [astro-ph/0303249].
- [39] H. Tashiro, PTEP **2014**, no. 6, 06B107 (2014).
- [40] Y. B. Zeldovich and R. A. Sunyaev, Astrophys. Space Sci., **4**, 301 (1969).
- [41] R. A. Sunyaev and Y. B. Zeldovich, Astrophys. Space Sci., **7**, 20 (1970).
- [42] R. Khatri, R. A. Sunyaev and J. Chluba, Astron. Astrophys. **540**, A124 (2012) [arXiv:1110.0475 [astro-ph.CO]].
- [43] J. B. Dent, D. A. Easson and H. Tashiro, Phys. Rev. D **86**, 023514 (2012) [arXiv:1202.6066 [astro-ph.CO]].
- [44] J. Chluba, A. L. Erickcek and I. Ben-Dayan, Astrophys. J. **758**, 76 (2012) [arXiv:1203.2681 [astro-ph.CO]].
- [45] R. A. Sunyaev and R. Khatri, Int. J. Mod. Phys. D **22**, 1330014 (2013) [arXiv:1302.6553 [astro-ph.CO]].